ÇUKUROVA UNIVERSITY
INSTITUTE OF NATURAL AND APPLIED SCIENCES

MSc THESIS

Kerem SALÇIN

A METHOD FOR BRAIN TUMOR CLASSIFICATION FROM MRI IMAGES USING DEEP LEARNING AND IMAGE ENHANCEMENT TECHNIQUES

DEPARTMENT OF ELECTRICAL AND ELECTRONICS ENGINEERING

ADANA-2019

ÇUKUROVA UNIVERSITY
INSTITUTE OF NATURAL AND APPLIED SCIENCES

A METHOD FOR BRAIN TUMOR CLASSIFICATION FROM MRI IMAGES USING DEEP LEARNING AND IMAGE ENHANCEMENT TECHNIQUES

Kerem SALÇIN

MSc THESIS

DEPARTMENT OF ELECTRICAL AND ELECTRONICS ENGINEERING

We certify that the thesis titled above was received and approved the award of degree of the Master of Science by the board of jury on

……..……	……..……..	..…..……..…….
Asst. Prof. Dr. Ercan AVŞAR	Assoc. Prof. Dr. Sami ARICA	Asst. Prof. Dr. Emine AVŞAR AYDIN
SUPERVISOR	MEMBER	MEMBER

This MSc Thesis is written at the Electrical and Electronics Engineering Department of Institute of Natural and Applied Sciences of Çukurova University.
Registration Number:

Prof. Dr. Mustafa GÖK
Director
Institude of Natural and Applied Science

This work was supported by Research fund of the Cukurova University under grant no FYL-2019-11415.

ABSTRACT

MSc THESIS

A METHOD FOR BRAIN TUMOR CLASSIFICATION FROM MRI IMAGES USING DEEP LEARNING AND IMAGE ENHANCEMENT TECHNIQUES

KEREM SALÇIN

ÇUKUROVA UNIVERSITY
INSTITUTE OF NATURAL AND APPLIED SCIENCES
DEPARTMENT OF ELECTRICAL AND ELECTRONICS ENGINEERING

Supervisor : Assist. Prof. Dr. Ercan AVŞAR
Year: 2019, Pages: 51
Juries : Asst. Prof. Dr. Ercan AVŞAR
: Assoc. Prof. Dr. Sami ARICA
: Asst. Prof. Dr. Emine AVŞAR AYDIN

Magnetic resonance imaging (MRI) is a useful method for diagnosis of tumors in human brain. In this work, MRI images have been analyzed to detect the regions containing tumor and classify these regions into three different tumor categories: meningioma, glioma, and pituitary. Deep learning is a relatively recent and powerful method for image classification tasks. Therefore, faster Region-based Convolutional Neural Networks (faster R-CNN), a deep learning method, has been utilized in this study. A publicly available dataset containing 3,064 MRI brain images (708 meningioma, 1426 glioma, 930 pituitary) of 233 patients is used for training and testing of the classifier. It has been shown that faster R-CNN method can yield an accuracy of 93.14% which is higher than the related work using the same dataset.

Keywords: Deep Learning, Convolutional Neural Network, Faster R-CNN, Classification, Brain Tumor

ÖZ

YÜKSEK LİSANS TEZİ

DERİN ÖĞRENME VE GÖRÜNTÜ İYİLEŞTİRME TEKNİKLERİ İLE BEYİN TÜMÖRLERİNİN MR GÖRÜNTÜLERİ KULLANILARAK SINIFLANDIRILMASI

Kerem SALÇIN

ÇUKUROVA ÜNİVERSİTESİ
FEN BİLİMLERİ ENSTİTÜSÜ
ELEKTRİK ELEKTRONİK MÜHENDİSLİĞİ ANABİLİM DALI

Danışman : Dr. Öğr. Üyesi Ercan AVŞAR
Yıl: 2019, Sayfa: 51
Jüri : Dr. Öğr. Üyesi Ercan AVŞAR
: Doç. Dr. Sami ARICA
: Dr. Öğr. Üyesi Emine AVŞAR AYDIN

Manyetik rezonans (MR) insan beynindeki tümörlerin tanısında yararlı bir yöntemdir. Bu çalışmada, tümör içeren bölgeleri tespit etmek ve bu bölgeleri üç farklı tümör kategorisinde (meningioma, glioma, pituitary) sınıflandırmak için MRI görüntüleri analiz edilmiştir. Derin öğrenme, görüntü sınıflandırma işleri için nispeten yeni ve güçlü bir yöntemdir. Bu nedenle, bu çalışmada bir deep learning metodu olan faster R-CNN kullanılmıştır. Sınıflandırıcı eğitimi ve testi için 233 hastanın 3064 beyin MR görüntülerini (708 meningioma, 1426 glioma, 930 pituitary) içeren kamuya açık veriseti kullanılmıştır. Faster R-CNN yöntemi ile % 93.14 oranında bir başarım sağlanmıştır ve bu oran aynı veri setini kullanan benzer çalışmalardan daha yüksektir.

Anahtar kelimeler: Derin Öğrenme, Konvolüsyonel Sinir Ağı, Faster R-CNN, Sınıflandırma, Beyin Tümörü

EXTENDED ABSTRACT

Brain tumor is reported to one of the deadliest type of cancer. There are numerous types of brain tumors. In this thesis, three types of tumors namely, glioma, meningioma and pituitary were examined. It is possible to diagnose tumors by means of various medical imaging modalities. Magnetic resonance imaging (MRI) is one these modalities and it provides a unique appearance in visualization of soft tissues with spatial resolution and contrast resolution. MRI images are visually observed by human experts for possible abnormalities. This procedure requires experience and prone to human-related errors. On the other hand, medical diagnosis systems exist that may help these experts in observing MRI images. Such systems basically involve processing of images and recognizing the related tumor area automatically. Therefore, the aim of this study is to develop a method that facilitates the detection and classification of tumors and to allow doctors to save time during diagnosis.

In this work, Faster R-CNN, a deep learning method, is used for detection of the brain tumous in MRI images. Deep learning is an artificial intelligence method which imitates the workings of the human brain in processing data and creating patterns for use in decision making. A Convolutional Neural Network (CNN) is a deep learning algorithm that gets an input image, gain importance to various objects in the image (learnable weights and biases) and distinguish one from the other. Therefore, they are mainly used for classifying images, clustering with similarities (photo searching) and making object recognition in scenes. It is possible to tell the class of the objects within an image via CNN; however, it does not return any location information. In order to find the object location, region based CNN (R-CNN) method has been developed. Faster R-CNN is an advanced version of R-CNN allowing for a classification with higher accuracy in a shorter time.

The public datasets for brain tumors were searched and a dataset consisting of 3064 brain MRI images of 233 patients with 3 different brain tumors is used in this thesis. Also, two spatial image enhancement techniques, namely, histogram equalization and unsharp masking, are applied to the same dataset. In order to observe the effects of image enhancement on classification performance, three different Faster R-CNN models are trained using original database images, images processed with histogram equalization and unsharp masking, respectively. All the programming has been carried out using Python programming language (v3.6.6) and Tensorflow (v1.12.0) library is used for training and testing of the classifier.

612 samples (constituting 20% of the dataset) are used for testing the faster R-CNN models. In tensorflow library, the minimum softmax probability value for assigning a class label to a detected tumor is set as 0.8 by default. This means that a tumor is left unclassified if the associated probability value is smaller than 0.8. By changing this probability threshold, a change in number of unclassified and misclassified samples is observed. Three confusion matrices belonging to three different threshold values (0.8, 0.66, and 0.5) are generated and five performance metrics (accuracy, precision, sensitivity, specificity, f-score) from these matrices are calculated. This procedure is repeated for three different classifiers and their results are compared. It has been observed that unsharp masking has positive effect and histogram equalization has negative effect on the performance. The highest classification accuracy (93.14%) is obtained with unsharp masked images when the threshold is 0.5.

ACKNOWLEDGEMENT

First, I would like to endless thank to my thesis supervisor Asst. Prof. Dr. Ercan AVŞAR for his constructive suggestions, corrections and support during my graduation process.

Also, I would like to thank to members of my Master Science thesis jury members, Assoc. Prof. Dr. Sami ARICA and Asst. Prof. Dr. Emine AVŞAR AYDIN for all respectable knowledge and experience.

Next, I would like to thank to faculty members of Çukurova University Electrical and Electronics Engineering Department.

Finally, I would like to special thank to my family, my father Hüseyin SALÇIN and my mother Songül SALÇIN who always supported to me in my life.

CONTENTS **PAGE**

ABSTRACT I
ÖZ II
EXTENDED ABSTRACT III
ACKNOWLEDGEMENT V
CONTENTS VI
LIST OF TABLES VIII
LIST OF FIGURES X
ABBREVIATIONS XII
1. INTRODUCTION 1
1.1. Brain and Brain Tumor 1
1.2. Magnetic Resonance Imaging 4
1.3. Deep Learning 4
1.4. Tensorflow 5
1.5. Problem Statement 6
1.6. Outline of the Thesis 7
2. RELATED WORKS 9
3. MATERIALS AND METHODS 17
3.1. Background 17
3.1.1. Convolution 20
3.1.2. Rectified Linear Unit (ReLU) 20
3.1.3. Pooling 21
3.1.4. Flattening 22
3.1.5. Fully Connected Layers 23
3.1.6. Softmax Function 24
3.2. Image Enhancement Methods 24
3.2.1. Unsharp Masking 25
3.2.2. Histogram Equalization 26

3.3. The Dataset 28
3.4. Training 29
4. RESULTS AND DISCUSSION 33
5. CONCLUSION AND FUTURE WORK 41
REFERENCES 43
CURRICULUM VITAE 51

LIST OF TABLES **PAGE**

Table 3.1. Comparison of Types of CNN 18
Table 3.2. Distribution of the dataset in three classes 29
Table 4.1. Confusion Matrix when threshold is 0.8 (63 samples unclassified) 34
Table 4.2. Confusion Matrix when threshold is 0.66 (48 samples unclassified) .. 34
Table 4.3. Confusion Matrix when threshold is 0.5 (35 samples unclassified) 34
Table 4.4. Performance metrics when threshold is 0.8 35
Table 4.5. Performance metrics when threshold is 0.66 35
Table 4.6. Performance metrics when threshold is 0.5 35
Table 4.7. Confusion Matrix when threshold is 0.8 (62 samples unclassified) 36
Table 4.8. Confusion Matrix when threshold is 0.66 (39 samples unclassified) .. 37
Table 4.9. Confusion Matrix when threshold is 0.5 (33 samples unclassified) 37
Table 4.10. Performance metrics when threshold is 0.8 (Unsharp Masking) 37
Table 4.11. Performance metrics when threshold is 0.66 (Unsharp Masking) 37
Table 4.12. Performance metrics when threshold is 0.5 (Unsharp Masking) 38
Table 4.13. Previous Works that Applies Various Deep Learning Techniques on This Dataset. 39

LIST OF FIGURES **PAGE**

Figure 1.1. Part of Brain 2
Figure 1.2. Images containing different types of brain tumors 4
Figure 3.1. Structure of CNN 19
Figure 3.2. Types of Rectified Linear 21
Figure 3.3. Example of Pooling 22
Figure 3.4. Example of Flattening 23
Figure 3.5. Structure of Fully Connected Layers 23
Figure 3.6. The Unsharp Masking Structure 26
Figure 3.7 Comparison of Unfilter Tumor Types vs Tumor Types Used Filter 28
Figure 3.8. Images containing different types of brain tumors 29
Figure 3.9. Labelling the Dataset by Using LabelImg Program 30
Figure 3.10. Structure of XML File 30
Figure 3.11. Total Loss Graph of the System 31
Figure 4.1. Detected and Classified Brain Tumors 33
Figure 4.2. Samples for Exceptional Test Cases 38

ABBREVIATIONS

AI	: Artificial Intelligence
ANFIS	: Adaptive Neuro-Fuzzy Inference System
ANN	: Artificial Neural Network
BoW	: Bag of Words
BPNN	: Back-Propagation Neural Networks
BraTS	: Brain Tumor Segmentation
BWT	: Berkeley Wavelet Transformation
CNN	: Convolutional Neural Network
CSF	: Cerebrospinal Fluid
CV	: Computer Vision
DWT	: Discrete Wavelet Transform
Faster R-CNN	: Faster Region-Based Convolutional Neural Network
FC	: Fully Connected
FFNN	: Feed Forward Neural Network
FFT	: Fast Fourier Transform
FN	: False Negative
FP	: False Positive
GLCM	: Gray level co-occurrence Matrix
ICA	: Independent Component Analysis
KNN	: K-Nearest Neighbors
LBP	: Local Binary Patterns
LDA	: Linear Discriminant Analysis
MKPC	: Multiple Kernel Probabilistic Clustering
MLP	: Multilayer Perceptron
MR	: Manyetik Rezonans
MRI	: Magnetic Resonance Imaging

MRMR	: Minimal Redundancy-Maximal Relevance
PCA	: Principle Component Analysis
RBF	: Radial Basis Function
R-CNN	: Region-Based Convolutional Neural Network
ReLU	: Rectified Linear Unit
ROI	: Region of Interest
RPN	: Region Proposal Network
SOM	: Self Organized Map
SVM	: Support Vector Machine
TN	: True Negative
TP	: True Positive
TPU	: Tensor Processing Units
UM	: Unsharp Masking
WHO	: World Health Organization

1. INTRODUCTION

1.1. Brain and Brain Tumor

Cancer is one of the major causes of death today. According to the reports of World Health Organization (WHO), it is estimated that 9.6 million people worldwide died of cancer in 2018 (www.who.int). 30-50% of these were preventable with early diagnosis. Among types of cancer, brain tumor is one of the deadliest one. According to statistics, in 2019, it is predicted that approximately 18000 adults can die from brain tumors (www.cancer.net).

A tumor which can be malign or benign starts when the DNA of cells is harmed. As a result of this change in genetic structure of the cells, the division of the cells becomes uncontrolled and eventually a mass is formed. A malign tumor is said to be cancerous. This means that if it is not diagnosed at early stages, it may grow and spread to different parts of the body. On the other hand, a benign tumor may grow too but it does not spread. Most of the times a benign tumor can usually be removed without much damage (www.cancer.net).

A tumor may grow on any tissue of the human body, including brain. The brain consists of 4 main section which are the cerebrum, the cerebellum, the brain stem and the meninges. The cerebrum is the biggest section of the brain consisting of two cerebral hemispheres on both sides of the brain. It is divided into four lobes with special functions. These are frontal lobe, parietal lobe, temporal lobe and occipital lobe. The frontal lobe controls expressive speech, reasoning, movement, emotions and problem-solving. The parietal lobe controls the sensations of touch. For instance, temperature, pressure and pain etc. And also, it controls calculation, parts of speech and visual-spatial orientation. The temporal lobe controls special senses like hearing, memory and the skill to understand written or spoken words. The occipital lobe controls vision. The cerebellum is positioned at the rear side of the brain under the cerebrum. It is responsible for controls functions, balance and coordination on the same part of the body. The brain stem is the section of the brain

that connects to the cerebellum and the spinal cord. It controls involuntary functions crucial for life. For example, breathing and beating of the heart etc. Messages for the functions which controlled by the cerebellum and cerebrum move through the brain stem to the body. The meninges are the membranes which protect and surround the brain and spinal cord. There are three meningeal layers which called the arachnoid, pia mater and dura mater. The cerebrospinal fluid (CSF) is made close the brain's center in the lateral ventricles. CSF circulates around spinal cord and the brain between the pia layers and arachnoid (www.cancer.net).

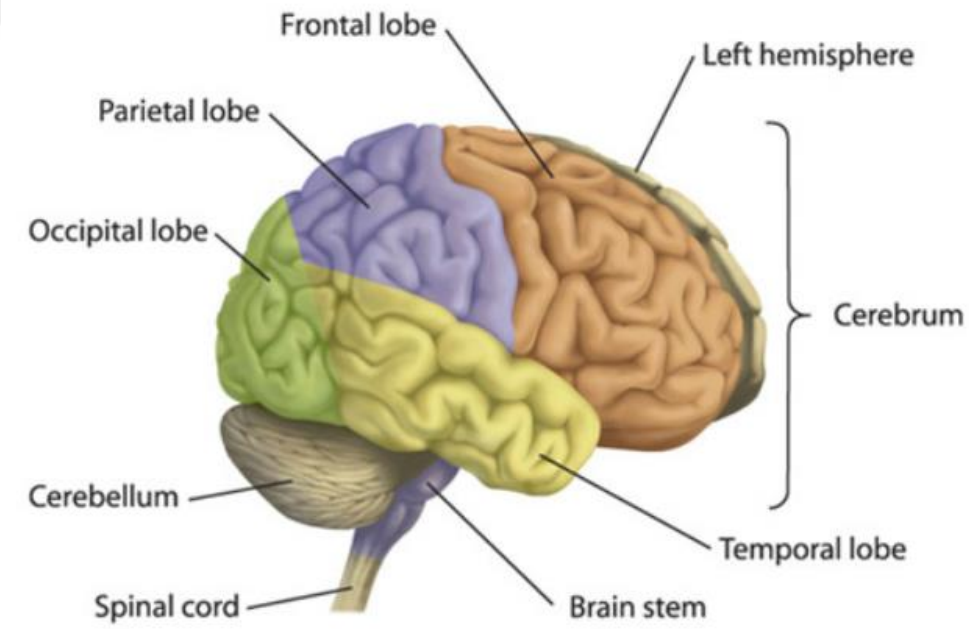

Figure 1.1. Part of Brain

There are numerous types of brain tumors. However, in this thesis three types of tumors namely, glioma, meningioma and pituitary were examined.

Glioma is a kind of tumor which occurs in the brain and spinal cord. Glioma starts in the gluey supportive cells (glial cells) which enclose nerve cells and help them work. Three kinds of glial cells can generate tumors. Gliomas are categorized according to the kind of glial cell included in the tumor which can help estimate how the tumor will act in time and the cures most likely to work. A glioma can impact brain functions and be life-threatening depending on its position and growth rate. Gliomas are one of the most widespread kinds of primary brain tumors. This type of glioma helps determine the treatment and prognosis. In general, glioma treatment choices contain experimental clinical trials, chemotherapy, surgery, radiation therapy and targeted therapy (www.mayoclinic.org).

A meningioma is a type of tumor that arises from the meninges — the membranes that surround the brain and spinal cord. Meningioma is the most widespread kind of tumor that forms in the brain. Most meningiomas grow very slowly, often over many years without any significant symptoms. But in some cases, their effects on adjacent brain tissue, nerves or vessels may cause serious disability. Meningiomas most usually seen in women, and are often found at older ages, but a meningioma may be seen at any age. Because most meningiomas grow slowly, often without any causing symptoms, they do not always necessary urgent cure and may be monitored over time (www.mayoclinic.org).

Pituitary tumors are anomalous growths which evolve in pituitary gland of the brain. Some pituitary tumors may cause decrement in the level of some hormones which adjust significant functions of your body. Most pituitary tumors are non-cancerous (benign) growths which is called adenomas. Adenomas remain in your pituitary gland surrounding tissues and don't spread to other sides of the body (www.mayoclinic.org).

1.2. Magnetic Resonance Imaging

High quality images of the body part under investigation can be obtained through magnetic resonance imaging (MRI). It is a frequently used method for the detection of brain tumors. Especially in brain imaging, the MRI method provides a unique appearance in visualization of soft tissues with spatial resolution and contrast resolution. It is a great advantage for MRI that it can be applied without giving no damage to the patient (Demirhan and Güler, 2014). Sample MRI images for three tumor types are given in Figure 1.2.

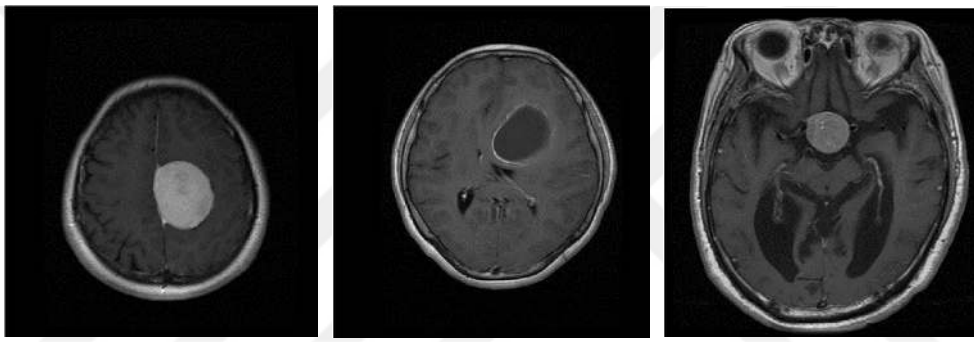

(a) (b) (c)

Figure 1.2. Images containing different types of brain tumors.
a) Meningioma b) Glioma c) Pituitary

1.3. Deep Learning

With the developing technology, various methods have been used in the detection and classification of brain tumors. In recent years, deep learning has come to the forefront with the development of artificial intelligence (AI). Deep learning is an AI method which imitates the workings of the human brain in processing data and creating patterns for use in decision making. It is a subset of machine learning in AI. Also known as deep neural network (www.investopedia.com). Deep learning lets computational models, which are composed of multiple processing layers, to learn representations of data with multiple levels of abstraction. These methods have significantly improved the latest technology in speech recognition, visual object

recognition, object detection and many other areas such as drug discovery and genomics. Deep learning explorers complex structure in big data sets by using the backpropagation algorithm to show how a machine should change its internal parameters that are used to compute the representation in each layer from the representation in the previous layer (LeCun, Bengio and Hinton ,2015).

A Convolutional Neural Network (CNN) is a deep learning algorithm that can get an input image, gain importance to various objects in the image (learnable weights and biases) and distinguish one from the other. Therefore, they are mainly used for classifying images, clustering with similarities (photo searching) and making object recognition in scenes.

The architecture of a CNN is similar to the connection model of neurons in the human brain and is inspired by the organization of visual cortex. Individual neurons respond to stimuli only in a limited region of the visual field known as the receptive field. A collection of such areas overlaps to cover the entire visual area (towardsdatascience.com).

The effectiveness of CNNs in image recognition is one of the main reasons why the world is awakened by the effectiveness of deep learning. They reinforce significant advances in computer vision (CV), which has specific applications for robotics, safety, self-driving automobiles, drones, medical diagnostics and treatments for the visually impaired (skymind.ai).

A typical CNN can decide whether an image contains an object but without its location information. On the other hand, region-based CNN (R-CNN), an extended version of CNN, is mainly used for locating objects in images.

1.4. Tensorflow

With the development of deep learning over time, various libraries have begun to be used to increase the accuracy and speed of processing datasets. One of these is the TensorFlow library which was launched as an open source project and is commonly used for machine learning research. TensorFlow library operates at major

scale and in different environments. TensorFlow uses dataflow graphs to represent computation, shared state and the operations changing that state. It maps the nodes of a data flow chart on multiple machines in a cluster and multiple computing devices, including multi-core processors, general-purpose GPUs, and specially designed ASICs known as Tensor Processing Units (TPUs) on one machine. That architecture adds flexibility to the application developer: whereas in previous "parameter server" designs the management of shared state is built into the system, TensorFlow enables developers to experiment with new optimizations and training algorithms. TensorFlow supports a variety of applications, with a focus on training and inference on deep neural networks (www.usenix.org).

1.5. Problem Statement

Today image processing plays an important role in medical field and medical imaging is a growing and challenging field. Medical imaging is advantageous in diagnosis of some diseases. Many people suffer from brain tumor which is a serious and dangerous disease. Medical imaging provides proper diagnosis of brain tumor (Deepa and Singh, 2016).

With the emergence of modern medical imaging modalities, the presence of most abnormalities in the human brain has completely been detectable. Among these modalities, MRI holds a special position in detection of brain tumors owing to its many advantages. But, it has been observed that manual detection of tumor, which is the current scenario in medical science, is a time consuming process. The manual detection delays the further treatment of the patient which acts as a risk to the patient's life. Also the medical procedure of biopsy, which involves insertion of medical instrument in the human brain, performed to collect information about the status of the tumor, also leaves its post-surgical effects on the patient. Thus, the detection and classification of the tumor may take hours. Taking a small step to overcome these limitations, a computer-aided diagnosis system, faster and more successful than manual ones, is proposed (Nilakshi and Bhattacharyya, 2018).

In this thesis, MRI brain images are analyzed using faster R-CNN method to detect and locate tumors in the images. This method has been chosen because it can perform classification with higher accuracy and speed than regular R-CNN. Besides, effects of image enhancement methods like histogram equalization and unsharp masking on the classification accuracy has been investigated. It should be noted that classification performance of Faster R-CNN method and these image enhancement techniques have not been investigated on this problem yet. All of the coding is performed with Python programming language (version 3.6.6) and implementation of deep learning model is done via tensorflow library (www.tensorflow.org).

The major contributions of the thesis may be listed as follows:

- Faster R-CNN method has been implemented using Tensorflow for classifying and locating the brain tumors.
- Effects of two different image enhancement methods (histogram equalization and unsharp masking) on the classification performance have been investigated.
- It has been observed that unsharp masking has positive effect on the performance. On the other hand, histogram equalization has negative effect.

1.6. Outline of the Thesis

The rest of this thesis is organized as follows. In chapter 2 related works are summarized for the classification of brain tumors. In chapter 3, materials and methods which are used in this thesis are explained. In chapter 4, results obtained from our study are presented and discussed. In chapter 5, our results are compared with the related works, and the contributions made in this thesis are discussed. Suggestions for future studies are presented in chapter 5.

2. RELATED WORKS

Brain tumor detection and classification problem has taken attention of many researchers for years. Therefore, various methods have been developed to solve this problem and most of these methods utilizes MRI images together with machine learning and image processing algorithms.

Among too many number of studies dealing with brain tumor detection problem, deep learning, artificial neural networks (ANN), support vector machines (SVM), Fourier transform and wavelet transform are the methods most commonly used. For example, SVM and Berkeley Wavelet Transformation (BWT) is used to detect normal and abnormal tissues from MRI brain images in the method proposed by Shree and Kumar (2018). Fast Fourier Transform (FFT) and Minimal Redundancy-Maximal Relevance (MRMR) techniques were used by Salem and Alfonso (2016) for the classification of brain tumors. Principle Component Analysis (PCA) and Radial Basis Function (RBF) were used by Kumar and Vijayakumar (2015) for the detection and classification of brain tumor MRI and better results were obtained. A multi-class brain tumor classification was proposed Sachdeva et. al. (2015). It consists T1-weighted MRI images and statistical texture and intensity features trained by ANN. The accuracy of this method was increased from 77% to 91% by reducing the size of the properties vector using PCA. In another study, a method for the detection and classification of brain tumors based on extracting shape, tissue and density characteristics from ROI, fragmented by multiple kernel probabilistic clustering (MKPC), were discussed by Sachdeva et al. (2013). And also, the extracted features were optimized by sachdeva et al. using linear discriminant analysis (LDA) and then trained by a deep neural network. A method for diagnosis of multiple sclerosis patients based on T2 MRI images were proposed Faro et. al. (2015). And this diagnosis was performed with 95% accuracy. In a new study, tissue properties were based on gray-level mapping. The statistical moments of the gray-level histogram were trained by using multilayer perceptron (MLP) by

Chato and Latifi (2017). The algorithm proposed by Lakshmi and Arivoli (2012) occurs four main sections. First section is pre-processing section. Next section is the extraction of the features. Thirdly is the classification of the features. Last and fourth section is detection the position of a brain tumor. The pre-processing section is to arrange the images to join the feature extraction section. In the second section, feature extraction method, like wavelet and GLCM, is used for the feature extraction. Then, these features are classified using adaptive neuro-fuzzy inference system (ANFIS) classification algorithm. In the last section, the tumor and tumor related fields are detected. A method that divides the images into cancerous and non-cancerous parts were proposed John et. al. (2012). The proposed algorithm contains three sections. In the first section, the images were converted to diverse grades of coefficients using discrete wavelet transform (DWT). Then the color intensity matrix was obtained. Using that matrix, features like solidarity, energy and some other features which related to the texture of images are extracted. In the final section, the type of class which each image belongs to is determined. A new method for brain tumor classification were proposed Cheng et. al. (2015). They have shown which using the increased tumor site as ROI may have a better effect on diagnosis and classification of brain tumor images. Three methods were used for feature extraction. These are intensity histogram, gray level co-occurrence matrix (GLCM) and bag-of-words (BoW). Between the other methods, bag-of-words (BoW) shows better result with 91.28% accuracy according to obtained results. How machine learning methods are useful in detecting tumor in MRI images were shown by Komal Sharma et al. (2013). They use two different methods which are Multilayer Perceptron (MLP) and Naive Bayes. The study using Multilayer Perceptron the success rate was 98.6%. And, the study using Naive Bayes the success rate was 97.6%. GLCM was used as a feature extractor. Texture feature like correlation, contrast, homogeneity were used to detect tumor characteristics. A system based on unsupervised learning Neural Network for brain tumor detection were proposed Goswami and Bhaiya (2013). Independent Component Analysis (ICA) were used for feature extraction and Self

Organized Map (SOM) were used for classification. To segment the brain into different tissue, segmentation was done by using k-means clustering algorithm. According to results, using this method 98.6 % accuracy was achieved. Neural network were used by the study of Ibrahim, Osman and Mohamed (2013) to classify MRI images. PCA (Principle component analysis) technique were used to reduce dimensionality in data. The dataset from CIPR database were used by them. For training and testing the algorithm 3x58 images were used. Accuracy of classification obtained from results was 96.33%. A system based on classification of brain cancer by means of artificial neural network were proposed by Joshi et. al. (2010). GLCM were used for feature extraction. For the pre-processing section was done by using image processing techniques like morphological operation, histogram enhancement. Neuro fuzzy classifier was used to classify the brain tumor into different classes. Their results have shown that their system was efficient enough to classify different brain tumor. A system built on Adaboost classifier to diagnose brain tumor in MR images were proposed by Prabin and Veerappan (2014).While classification was done using the Adaboost classifier, the wavelet transform and the level set method were used for feature extraction. Their results show that the accuracy rate of Adaboost classifier is better than compared tumor classification methods like Radial Basis Function (RBF) and Feed forward neural network (FFNN). And also, PCA method was used for dimensionality reduction. A method based on Adaboost classifier to detect brain tumors in MR images Ghanavati et al. (2012). Gadolinium contrast agent were used for image modalities. Intensity, deformation, shape and texture feature were used as the classification feature. Training and testing were perform on the multimodal MRI images. The results showed good performance with 90.11% accuracy. A system based on neural network based Adaboost algorithm to detect a tumor in brain MRI were proposed by Babu and Begum (2015). An improved patient self-reliant tumor clustering scheme were proposed using Adaboost procedure. Brain Tumor Segmentation (BraTS) 2012 dataset was used as a dataset. The results demonstrate that segmented results are more stable and show

average performance for patients. A system based on brain tumor detection in magnetic resonance imaging where they have used Back-Propagation Neural Networks (BPNN) and K-Nearest Neighbors (KNN) as a classifier were proposed by Gadpayle and Mahajani (2013). GLCM were used for feature extraction. The parameters were obtained like Dissimilarity, Entropy, Contrast, Homogeneity and Inverse Difference Moment by using GLCM. The Results demonstrate that BPNN has 72.5% and KNN has 70% accuracy for unseen images.

A technique called Fuzzy partition entropy with genetic algorithm were proposed by Yu and Fan (2008). Although they had chosen optimal parameters, practical implementation was difficult. Texture and automatic segmentation with seeded region growing algorithm to determine abnormal tissues in brain MRI images were proposed by Kumar and Mehta (2011). However, they consumed much time. Symmetry analysis algorithm to detect the stages of disease were implemented by Roy and Bandyopadhyay (2012). Brain tumor detection system using K-means clustering technique with BPN Classifier were proposed by Meenakshi and Anandhakumar (2012). Different segmentation techniques was applied by Haritha (2016), such as Local Binary Patterns (LBP), K-means, Morphological operations along with edge detection. If compare the order of the application, LBP, k-means and edge detection accuracy were great, respectively. Automatic brain tumor detection system with the help of preprocessing, morphological operations and threshold segmentation techniques were introduced by Akram and Anam (2011) to predict brain tumor. A system to identify the location of brain tumor were proposed by Neda and Hamid (2012). Thus, they segmented the brain images with better results. A segmentation algorithm were proposed by Debnath and Tai (2011) to detect abnormal tissues in brain. A fuzzy classifier to detect abnormal cells using biochemical features were proposed by Ouseph and Shruti (2016). A segmentation method on convolution neural network were proposed Pereira et al. (2016) to identify tumor in brain.

As one of the machine learning methods, deep learning is relatively recent and a popular method. It is highly effective in solving medical image analysis problems including lung cancer diagnosis (Sun,Zheng, and Qian, 2016), tibial cartilage segmentation (Prasoon et al., 2017) and brain tumor detection (Havai et al., 2017; Işın, Direkoğlu, and Şah, 2016; Zhang et al., 2016; Urban et al., 2014). Using deep learning methods, automatic segmentation has been successfully performed on large amounts of MRI images (Havai et al., 2017; Işın, Direkoğlu, and Şah, 2016). In particular, CNN-based algorithms for automated MRI segmentation for brain tumor yielded successful results by distinguishing distinctive features (Urban et al., 2014).

Between the deep learning based approaches for brain tumor segmentation CNN-based methods outperformed others. In other words, CNN has become a preferred methodology and has been widely applied in various medical image tasks and has shown promising results (Urban et al, 2014; Radiation Oncology Branch, 2018; Chen et al., 2018; Chen et al., 2018; Cullen and Avants, 2018; Iqbal et al., 2018; Wachinger, Reuter and Klein, 2018: Zhao et al., 2018).

In order to grade brain tumors, various layers of CNNs are trained in the method by Pan et al. (2015). However, they report that low number of training data causes problems in classifying the brain tumors. Pereira et al. (2016) applied to brain tumor segmentation using 3 x 3 convolution filters in MRI scans. The use of small filters is a form of regulation to prevent over-fitting by minimizing the number of parameters in the network. Using the BraTS validation tool, they achieved Dice scores of 88% for whole tumor, 83% for tumor core, and 77% for active tumor. One of the most successful examples in the context of MRI brain tumor segmentation is the work of Havaei et al. (2015). A cascaded two pathway CNN architecture that removes little and bigger sized patches at the same time were proposed by them. The cascaded CNN processes regional and universal details of the brain MRI. While being centered at the same point, the regional and universal patches are removed. A CNN processes the universal patches first, and then combined with the local patches

and fed to a two-way CNN with 7x7 filters in one path and 13 × 13 filters in the other. To avoid class unbalance, they propose a two phase training. It consists on training the CNN first with a balanced distribution of classes and then training it with a representative distribution of the original images. Kamnitsas et al. (2015) also propose a multi-path network but use 3D filters. When using these networks in a fully connected manner, the pooling layers cause a loss of resolution in the output. Because of this loss of resolution, it is common to add an upsampling path with skip connections to aid in recovering high-resolution detail (Long, Shelhamer and Darrell, 2015). The popular U-Net architecture uses a symmetric network with downsampling followed by upsampling with skip connections in between (Isensee et al, 2017; Ronneberger, Fischer and Brox, 2015). An exciting but relatively undiscovered alternative to downsampling and upsampling is the use of dilated convolutions (Yu and Koltun, 2016; Yu, Koltun and Funkhouser, 2017). Dilated convolutions let the network to look at bigger comprehensive areas without an exponential rise in parameters. They have been demonstrated to achieve perfect results on overall image segmentation datasets. But, the implementation of dilated convolutional neural networks to medical image analysis has not achieved enough success. In recent study, a modification of the Dilated Residual Network by Yu et al. (2017) was introduced and it was applied to brain tumor segmentation in MRI scans. The network was evaluated by training and testing on the BraTS 2017 challenge dataset (Bjoern et al, 2015). To address the severe label imbalance in the dataset, a balanced patch-based sampling approach was adopted for training. An ablation study which confirms the importance of residual connections in the network design were performed.

11-layers deep, three dimensional Convolutional Neural Network for the challenging task of brain lesion segmentation were presented by Kamnitsas et al. (2017). Dual pathway architecture to incorporate both regional and bigger contextual information were applied by them. At the last part, a 3D fully connected conditional random area was used for soft segmentation, which effectively extract false

positives. Similarly, Havaei et. al. (2017) simultaneously exploited local contextual features, together with universal contextual features by using two different CNN paths, unified at the last layer.

This study is a unique study for the detection and classification of brain tumors using tensorflow library. The study is not only limited to the detection and classification of brain tumors but also serves as an example for the detection and classification of tumors in other parts of the body. Dissemination of the application will make significant contributions to the literature.

3. MATERIALS AND METHODS

3.1. Background

It is possible to tell the class of the objects within an image via CNN; however, it does not return any location information. In order to find the object location R-CNN method has been developed. In R-CNN, some candidate regions of the image are selected with some region proposal functions. These regions are cropped and resized to be classified by CNN method. One improved method of R-CNN is fast R-CNN where the entire image is processed rather than cropping the image and resizing the cropped parts. Region proposal functions used in fast R-CNN as well. But unlike CNN, these regions are not processed directly; CNN features corresponding to each region proposal are pooled by fast R-CNN method. Generation of region proposals in a faster and better way is achieved by region proposal network (RPN). Faster R-CNN method introduces RPN directly in the network thereby enables a higher classifier performance (Ezhilarasi and Varalakshmi, 2018). Comparison of these methods are summarized in Table 3.1.

Table 3.1. Comparison of Types of CNN

METHOD	PROPERTIES	APPROXIMATE TIME FOR PREDICTION (sec)	DISADVANTAGES
CNN	A number of regions are created from the image. Then each reagion is classified separately.	-	Number of required regions is high for an accurate prediction. As a result, the computation time is high.
R-CNN	The regions are generated in a selective manner. About two-thousand regions are created per image.	40-50	Three different classifiers are used for class assignment. Besides, each of the regions are processed separately. This results in a high computation time.
Fast R-CNN	Related feature maps are extracted by feding the image only one time to the CNN. The three classifiers in R-CNN method are meged and only the selected feature maps are used for predictions.	2	Even though the number of classifiers is reduced, the search algorithm for selecting feature maps slows down the procedure.
Faster R-CNN	Region proposal network, a very fast method, is utilized instead of selective search.	0.2	Due to the cascaded systems, the error in one of the systems is passed to the next one. Thus, performance of a system may be low because of a bad input.

The process of building a CNN involves six main steps: Convolution, Rectified linear unit (ReLU), Pooling, Flattening, Fully connected layers, and Softmax function (Figure 3.1.). At the initial step, a number of convolution filters are applied to the input image to activate certain features from the images. In order to increase the training speed, negative values are mapped to zero and positive values remained unchanged in ReLU step. The purpose of pooling step is to simplify the output by performing nonlinear downsampling, and hence reducing the number of parameters that the network needs to learn about. These three operations are repeated over tens or hundreds of layers, with each layer learning to detect different features. In the flattening step, all two-dimensional arrays are transformed into one single linear vector. Such a process is needed for fully connected layers to be used after convolutional layers. Fully connected layers are able to combine the entire local features of the previous convolutional layers. The procedure is finished with application of softmax function to provide the final classification output.

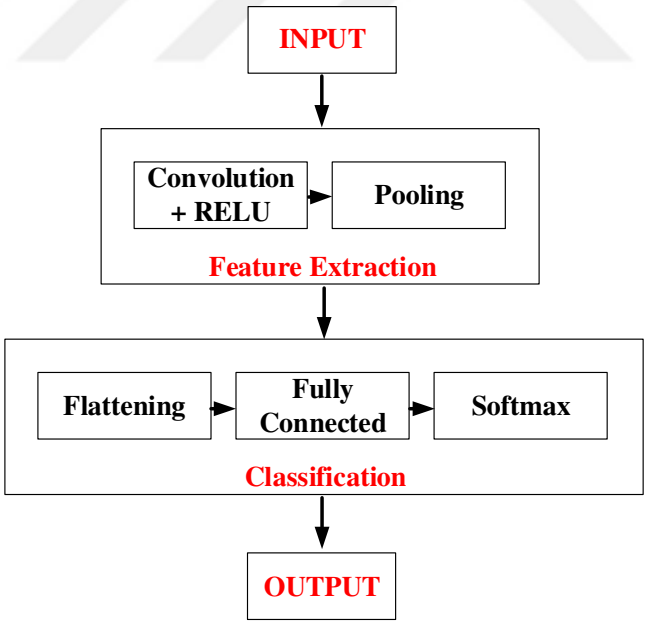

Figure 3.1. Structure of CNN

3.1.1. Convolution

Convolution of two functions is basically rotating one function by $180^{\mathbf{o}}$ about its origin and sliding it past the other. At each slidig step, a mathematical calculation is performed. Mathematically, this operation is defined as:

$$f(t) * h(t) = \int_{-\infty}^{\infty} f(\tau)h(t-\tau)\, d\tau \tag{3.1}$$

$$= \int_{-\infty}^{\infty} f(t-\tau)h(\tau)\, d\tau \tag{3.2}$$

Here the minus sign is for the rotating step, t is the displacement at each sliding step, and τ is a dummy variable for integration. The result of this convolution operation is named as feature map (other known names are activation map and convolved feature map). The input functions of the equation (3.1) are the input image and the convolution filter. The input image is the one being processed and classified. The convolution filter (also known as kernel matrix or feature detector) is an $m \times m$ matrix where m is an odd integer and is usuall equal to three or seven.

At the end of the convolution step, the size of the image is reduced, hence it becomes easier and faster to carry out the upcoming steps. Even though some features of the input image are lost, the principal features significant for the overall detection are preserved. Also, due to the high number of feature maps created, total loss of important information in the image is kept low.

3.1.2. Rectified Linear Unit (ReLU)

This step takes its name from the non-linear rectifier functions that are applied to improve the nonlinearity in the network. By the nature of the object detection problem, the objects in the images are not linear to each other. Therefore, this problem should be treated as a non-linear problem and it is accomplished by the

rectifier functions. ReLU layer involves an activation function that is applied to the entire data. The obtained matrix after this step is named as rectified feature map. Some rectifier functions are given in figure 3.2. and the related equations are provided in equations 3.3, 3.4 and 3.5.

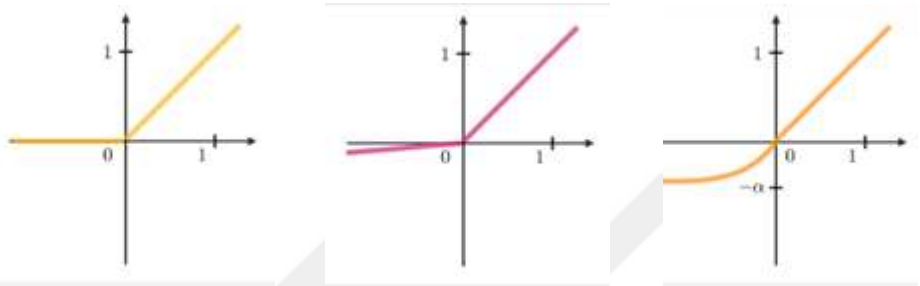

(a) (b) (c)

Figure 3.2 Types of Rectified Linear Unit a) ReLU b) Leaky ReLU c) ELU

ReLU: $g(z) = \max(0, z)$ (3.3)

Leaky ReLU: $g(z) = \max(\epsilon z, z) \quad with\ \epsilon \ll 1$ (3.4)

ELU: $g(z) = \max(\alpha(e^z - 1), z) \quad with\ a \ll 1$ (3.5)

3.1.3. Pooling

Regardless of the size, rotation, illumination and location of the object in the image, the CNN should be able to detect it. This concept is known as spatial invariance which is accomplished by the pooling step in training of a CNN model.

In the pooling procedure, a pooling filter is shifted over the entire input matrix with predefined size of steps. At each step, output of the filter is recorded to generate a pooled feature map. Conventionally, steps are chosen to be equal to the size of the pooling filter so that pooling is performed on the non-overlapping regions of the input matrix. According to the type of the pooling filter different types of pooling may be obtained such as average pooling, max pooling and min pooling. An example of max pooling with 2x2 filters and a stride of 2 is illustrated in Figure 3.3.

The pooling step may be considered as a dimensionality reduction method as the dimension of the resulting pooled feature map is smaller than the input feature map. So it makes contribution to processing speed of the algorithm. Furthermore, max pooling keeps the significant features of the image. These properties are important for preventing overfitting which is likely to occur when too much irrelevant information is provided to the CNN.

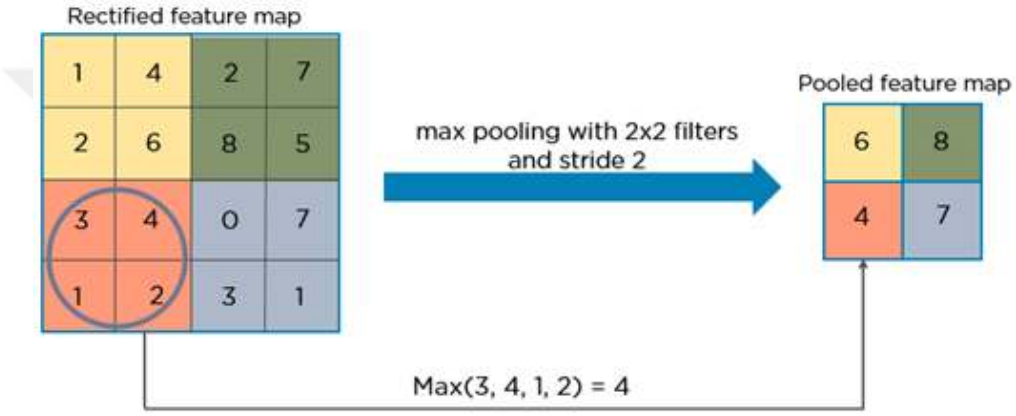

Figure 3.3. Example of Pooling

3.1.4. Flattening

The obtained pooled feature map in the previous step is converted into a one dimensional vector. This process is named as flattening. The flattened vector is then sent to fully connected layer for classification of the images.

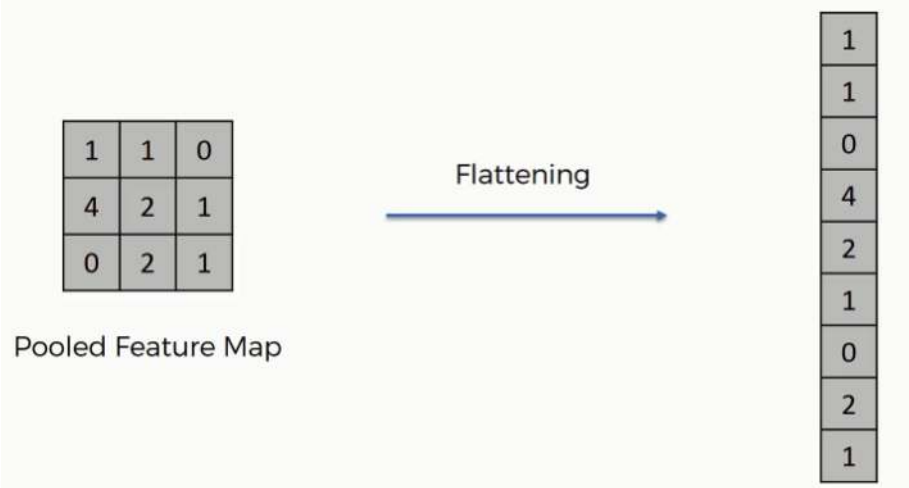

Figure 3.4. Example of Flattening

3.1.5. Full Connected Layers

The term fully connected means that every neuron in a layer has connection to all neurons in the following layer (Figure 3.5). The principle of fully connected layers is same as the well-known multilayer perceptron. Basically, the flattened feature vectors are used as input to a fully connected neural network. Optimization of the weights in the network and minimization of the prediction error is done via backpropagation. Eventually, class scores for the flattened vectors are calculated at the output of the network.

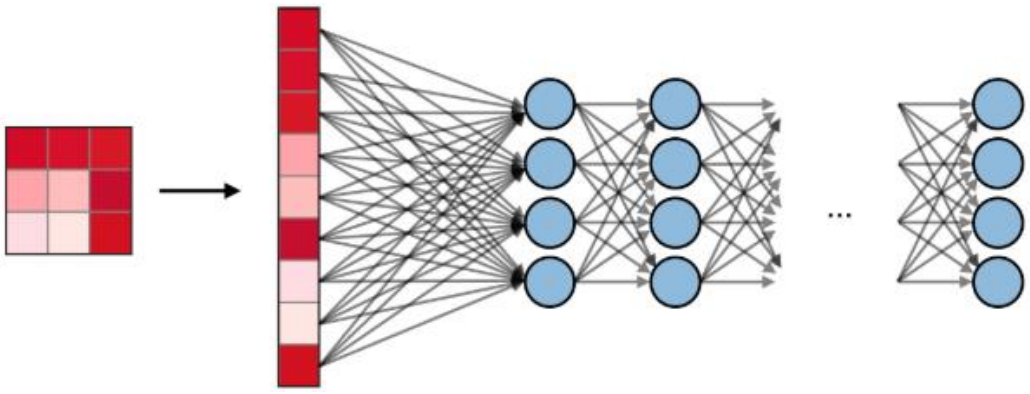

Figure 3.5. Structure of Fully Connected Layers

3.1.6. Softmax Function

The obtained scores at the end of the fully connected layers are real-valued numbers. However, these scores should be scaled to the interval [0,1]. Such a scaling is necessary for assigning a probability belonging to a particular class for the input vector. Therefore, at the output of the fully connected layers, softmax function (Equations 3.6 and 3.7) is used as the activation function and sum of the resulting scores is scaled to one.

$$\sigma: \mathbb{R}^K \rightarrow (0,1)^K \tag{3.6}$$

$$\sigma(z)_j = \frac{e_j^z}{\sum_{k=1}^{K} e_k^z} \quad for\ j = 1, \ldots, K. \tag{3.7}$$

3.2. Image Enhancement Methods

Most of the times, application of image processing methods to an image involves series of steps. In order to provide more successful output between the steps, image enhancement methods are utilized. In other words, image enhancement methods improve the information contained in an image. This improvement is not about quantitative measures, but it is about visual quality of the image. So, evaluation of image enhancement is an objective procedure. Also, some image enhancement methods may reveal the details in an image that are not visually observable before the enhancement. In order to accomplish this, some features of the image, such as contrast, brightness or gray level distribution, are modified. Morphological operations, median filtering, unsharp masking, histogram equalization, spatial filtering are some of the well-known image enhancement methods. The selection of the image enhancement method should be problem-specific. This means that all the methods may not be suitable for a particular problem.

It is possible to categorize the image enhancement methods in two broad categories: (*i*) Spatial Domain or (*ii*) Frequency Domain. Whatever the enhancement method is, the pixel intensities of the input image is modified at the end. In the spatial

domain methods, this modification is performed directly on the image pixels. On the other hand, the frequency domain methods invole transforming the image into frequency space representation. This is accomplished by computation of Fourier Transform of the image. The transformed image is processed and then transformed back to spatial domain representation by Inverse Fourier Transform.

In this work, two spatial domain methods are applied to MRI images and their effects on detection accuracy is observed. These methods are *unsharp masking* and *histogram equalization*. Technical details about these methods are given below.

3.2.1. Unsharp Masking

The main purpose of unsharp masking is to sharpening the edges in the input image. In this method a blurred version of the input image is subtracted from the original image. This is analogous to high-pass filtering the original image. The output of the filter is named as unsharp mask and is multiplied by a coefficient for tuning the sharpening amount. Then output of this multiplication step is added to the original image and a sharpened version of the image is obtained. This procedure is illustrated in Figure 3.6.

The mathematical relation for unsharp masking method is given in equation 3.8.

$$s_{i,j} = x_{i,j} + \lambda * \mathcal{F}(x_{i,j}) \tag{3.8}$$

Here, $x_{i,j}$ is the original intensity level at the coordinate (i,j), $F(.)$ denotes the highpass filtering, λ is a parameter for tuning the amount of sharpening ($\lambda \geq 0$), and $s_{i,j}$ is the resulting sharpened pixel at (i,j). As the value of λ is increased a more sharpened image is obtained at the end.

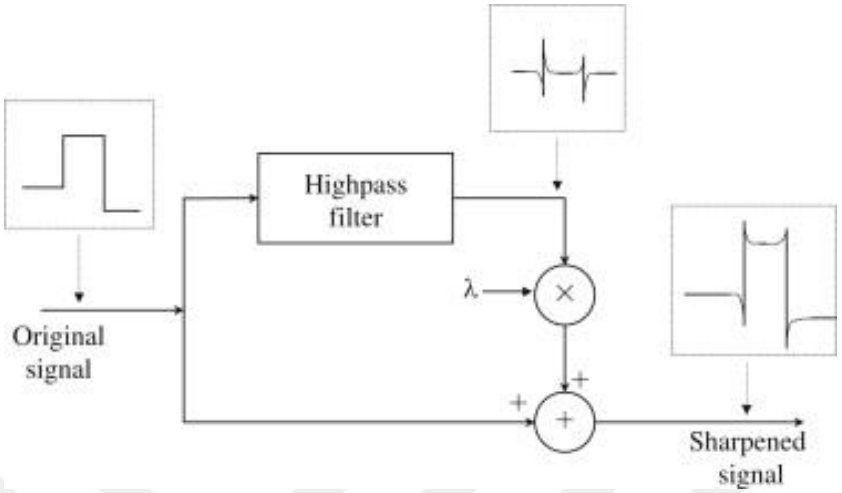

Figure 3.6. The Unsharp Masking Structure

3.2.2. Histogram Equalization

One of the most common image enhancement methods is histogram equalization. Basically, the aim in this method is to enhance contrast by adjusting pixel intensities.

Consider an input image whose histogram is skewed to one side. Since intensities of dark pixels are low and bright pixels are large, the histogram will be skewed to left side for a dark image and right side for a bright image. For an 8-bit image, histogram equalization stretches the skewed histogram across the entire spectrum of pixels (0 – 255), so the histogram of the resulting image will be closer to uniform distribution than the histogram of the input image. In that case compressed details of the input image become visible.

There are numerous variations of histogram equalization but the basic global enhancement version is used in this work. In this method, intensity level *j* for each of the pixels is mapped to a new pixel value (*K*) by using the formula given in equation 3.9.

$$K = \sum_{i=0}^{j} \frac{N_i}{M} \qquad j = 0,1,2,\ldots\ldots,M-1 \tag{3.9}$$

Here, M is the total number of pixels in the image and N_i is the total number of pixels with intensities equal to or less than j. Using histogram equalization method, a find gray level transformation T is found that transforms image f such that the histogram of the processed image T(f) is equalized.

Sample images from dataset as well as results of these image enhancement methods are illustrated in Figure 3.7.

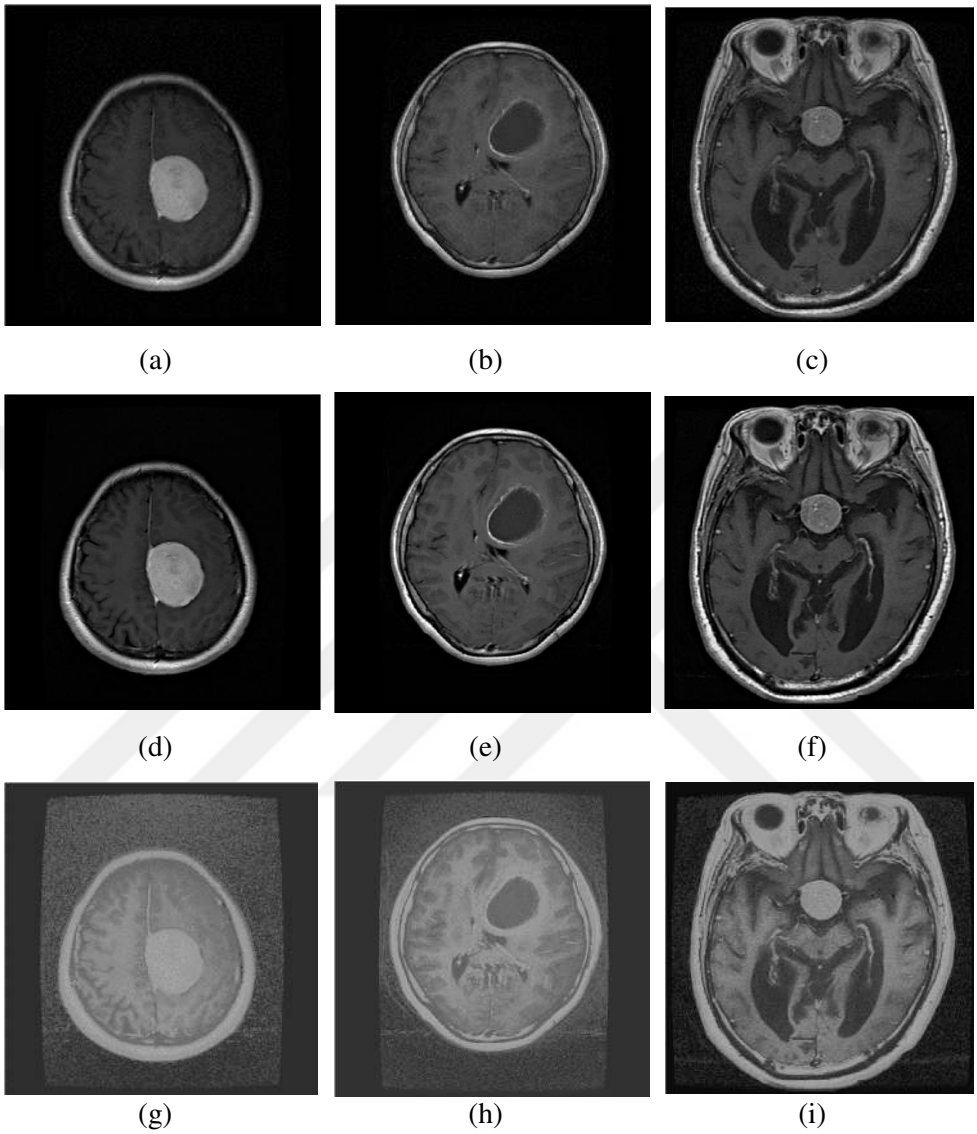

(a) (b) (c)

(d) (e) (f)

(g) (h) (i)

Figure 3.7. Sample images from the dataset (top row) and results of unsharp masking (middle row) and histogram equalization methods (bottom row). First column is meningioma, second column is glioma and the third column is pituitary

3.3. The Dataset

The brain image dataset contains 3,064 MRI slices from 233 patients. Each of these images contains one of the three types of brain tumors: meningioma, glioma,

or pituitary. The images have an inplane resolution of 512×512 with pixel size 0.49×0.49 mm^2. The slice thickness is 6 mm and the slice gap is 1 mm (Federer et al., 2018). Sample images from each of the classes are shown in Figure 3.8. and distribution of the images having these tumor types is given in Table 3.2.

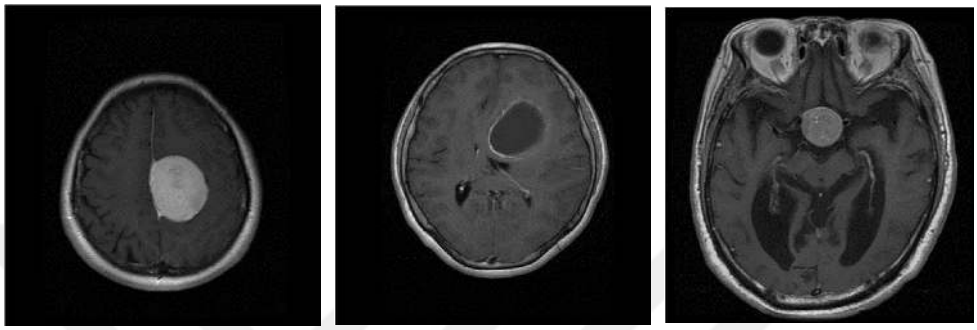

(a) (b) (c)

Figure 3.8. Images containing different types of brain tumors. a) Meningioma b) Glioma c) Pituitary

Table 3.2. Distribution of the dataset in three classes

Tumor Type	**Number of Images**
Meningioma	708
Glioma	1426
Pituitary	930
Total	**3064**

3.4. Training

In order to train and test the faster R-CNN classifier, the tumor locations in all of the images should be labeled and saved to a file. For this purpose, graphical image annotation tool called LabelImg (github.com) is used (Figure 3.9). Labelimg is written in Python and uses Qt for its graphical interface. Annotations are saved as XML files in PASCAL VOC format, the format used by ImageNet (Figure 3.10) (www.image-net.org).

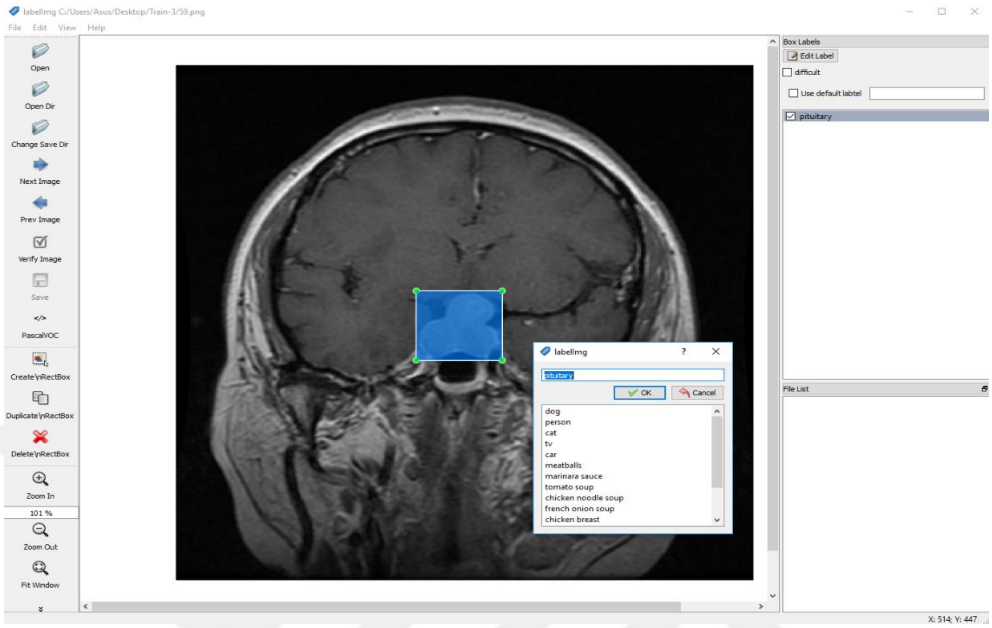

Figure 3.9. Labelling the Dataset by Using LabelImg Program

```
<annotation>
    <folder>Train-3</folder>
    <filename>59.png</filename>
    <path>C:/Users/Asus/Desktop/Train-3/59.png</path>
    <source>
        <database>Unknown</database>
    </source>
    <size>
        <width>1069</width>
        <height>948</height>
        <depth>1</depth>
    </size>
    <segmented>0</segmented>
    <object>
        <name>pituitary</name>
        <pose>Unspecified</pose>
        <truncated>0</truncated>
        <difficult>0</difficult>
        <bndbox>
            <xmin>466</xmin>
            <ymin>397</ymin>
            <xmax>585</xmax>
            <ymax>505</ymax>
        </bndbox>
    </object>
</annotation>
```

Figure 3.10. Structure of XML File

After labelling process, 80% of the images with each of the tumor types are randomly selected to form the training data and the remaining 20% is left for testing. A faster R-CNN model is trained on the training data. The parameters regarding the model are as follows:

- **Learning rate:** 0.0002
- **Momentum constant:** 0.9
- **Batch size:** 1
- **Number of iterations:** 150,000
- **Softmax neurons:** 3
- **Max-pool kernel size:** 2
- **Max-pool stride:** 2

The loss function that is being minimized during training is provided in Figure 3.11. At the beginning of the training, very high loss rate is observed. For example, in the first iteration total loss is approximately 90%. After 140.000 iterations, total loss is decreased to a value about 2%. This is an expected situation indicating that the algorithm performs learning process. Basically, two different loss functions are minimized in this problem. One is related to correct classification rate and the other one is related to location of the correctly classified object. Since graphs of both functions are similar, only Total Loss graph is given here as sum of these two functions.

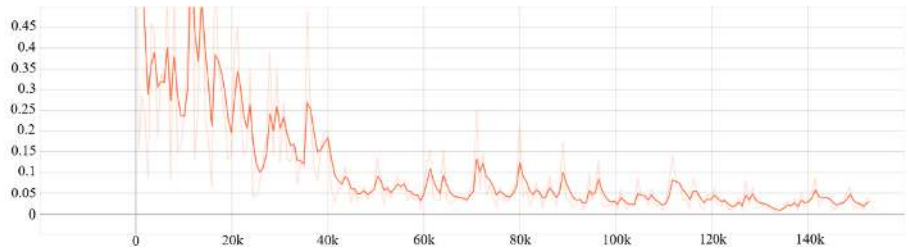

Figure 3.11. Total Loss Graph of the System

4. RESULTS AND DISCUSSION

612 samples (constituting 20% of the dataset) are used for testing the faster R-CNN model. For each test image three parameters are returned: (*i*) class label of the detected tumor, (*ii*) probability of the tumor being in that class and (*iii*) location of the tumor. Sample classification results are shown in Figure 4.1.

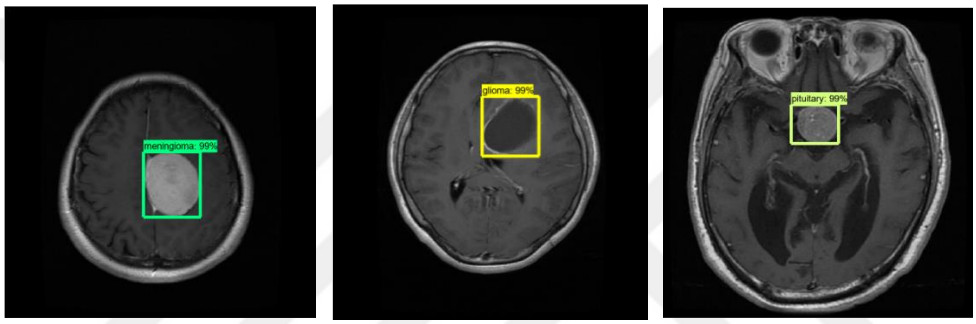

(a) (b) (c)

Figure 4.1. Detected and classified brain tumors. a) Meningioma b) Glioma c) Pituitary

In tensorflow library, the minimum softmax probability value for assigning a class label to a detected tumor is set as 0.8 by default. This means that a tumor is left unclassified if the associated probability value is smaller than 0.8. By changing this probability threshold, a change in number of unclassified and misclassified samples is observed. Three confusion matrices belonging to three different threshold values (0.8, 0.66, and 0.5) are given in Tables 4.1.,4.2. and 4.3, respectively.

Table 4.1. Confusion Matrix when threshold is 0.8 (63 samples are unclassified)

		PREDICTED			UNCLASSIFIED
		Meningioma	Glioma	Pituitary	
ACTUAL	Meningioma	129	0	4	8
	Glioma	5	237	2	41
	Pituitary	2	1	169	14

Table 4.2. Confusion Matrix when threshold is 0.66 (48 samples are unclassified)

		PREDICTED			UNCLASSIFIED
		Meningioma	Glioma	Pituitary	
ACTUAL	Meningioma	130	0	6	5
	Glioma	6	244	2	33
	Pituitary	3	1	172	10

Table 4.3. Confusion Matrix when threshold is 0.5 (35 samples are unclassified)

		PREDICTED			UNCLASSIFIED
		Meningioma	Glioma	Pituitary	
ACTUAL	Meningioma	133	0	4	4
	Glioma	6	251	2	26
	Pituitary	3	1	177	5

Five performance metrics, given in equations 4.1-4.5, are calculated using the classification results. Computation of these quantities requires clear definition of the confusion matrix elements, that are True Positive (TP), True Negative (TN), False Positive (FP) and False Negative (FN). Since values of these elements change according to the reference class label, three different values for each of the performance metrics are calculated for each of the confusion matrices in Tables 4.1., 4.2. and 4.3. The related results are given in Tables 4.4., 4.5. and 4.6.

Accuracy = (TP+TN)/(TP+TN+FP+FN) (4.1)

Precision =TP / (TP + FP) (4.2)

Sensitivity = TP / (TP + FN) (4.3)

Specificity = TN / (FP + TN) (4.4)

F-score = 2*TP /(2*TP + FP + FN) (4.5)

Table 4.4. Performance metrics when threshold is 0.8

Reference Class	Accuracy	Precision	Sensitivity	Specificity	F-Score
Meningioma	**0.8742**	0.9485	**0.9149**	0.9851	0.9314
Glioma	**0.8742**	**0.9957**	0.8316	**0.9969**	0.9063
Pituitary	**0.8742**	0.9657	0.9086	0.9859	**0.9363**

Table 4.5. Performance metrics when threshold is 0.66

Reference Class	Accuracy	Precision	Sensitivity	Specificity	F-Score
Meningioma	**0.8922**	0.9353	0.9220	0.9809	0.9286
Glioma	**0.8922**	**0.9959**	0.8561	**0.9969**	0.9207
Pituitary	**0.8922**	0.9570	**0.9247**	0.9812	**0.9405**

Table 4.6. Performance metrics when threshold is 0.5

Reference Class	Accuracy	Precision	Sensitivity	Specificity	F-Score
Meningioma	**0.9166**	0.9366	0.9433	0.9809	0.9399
Glioma	**0.9166**	**0.9960**	0.8807	**0.9969**	0.9348
Pituitary	**0.9166**	0.9672	**0.9516**	0.9859	**0.9593**

It is clearly seen from the confusion matrices (Tables 4.1, 4.2 and 4.3) that the number of unclassified samples decreases as the decision threshold is decreased. Also, the related performance measures are improved by decreasing the threshold. Considering the accuracy values in Tables 4.4., 4.5. and 4.6, 87.42% of the images

may correctly be classified when the decision threshold is set to 0.8 and this accuracy is increased to 91.66% when the threshold is set as 0.5. This means that, even though the output probability of the classifier is relatively low for some of the images, the tumor can be correctly detected. On the other hand, majority of the unclassified and misclassified samples belong to "Glioma" class, meaning that the classifier cannot learn this class as effectively as the other two. However, specificity value related to "Glioma" class is the highest for three of the thresholds.

As mentioned earlier, histogram equalization and unsharp masking methods are applied to input images and their effects on the classification performance is observed. Since the results related to histogram equalization are very low when compared to the ones in Tables 4.1, 4.2 and 4.3, they are not reported explicitly. However, application of unsharp masking improves the classification performance. The confusion matrices and the associated performance metrics are presented in Tables 4.7-4.12. As in the case of no image enhancement method, decreasing the threshold improves the correct classification rate, eventually yielding a maximum accuracy of 93.14% when the threshold is set as 0.5.

Table 4.7. Confusion Matrix when threshold is 0.8 (62 samples are unclassified)

	PREDICTED				**UNCLASSIFIED**
ACTUAL		Meningioma	Glioma	Pituitary	
	Meningioma	129	1	2	9
	Glioma	4	239	2	40
	Pituitary	2	0	171	13

Table 4.8. Confusion Matrix when threshold is 0.66 (39 samples are unclassified)

		PREDICTED			UNCLASSIFIED
		Meningioma	Glioma	Pituitary	
ACTUAL	Meningioma	133	2	2	4
	Glioma	4	251	2	28
	Pituitary	1	0	178	7

Table 4.9. Confusion Matrix when threshold is 0.5 (33 samples are unclassified)

		PREDICTED			UNCLASSIFIED
		Meningioma	Glioma	Pituitary	
ACTUAL	Meningioma	134	2	1	4
	Glioma	3	258	2	22
	Pituitary	1	0	178	7

Table 4.10. Performance metrics when threshold is 0.8

Reference Class	Accuracy	Precision	Sensitivity	Specificity	F-Score
Meningioma	**0.8807**	0.9555	0.9149	0.9873	0.9348
Glioma	**0.8807**	**0.9958**	0.8366	**0.9969**	0.9105
Pituitary	**0.8807**	0.9771	**0.9194**	0.9859	**0.9474**

Table 4.11. Performance metrics when threshold is 0.66

Reference Class	Accuracy	Precision	Sensitivity	Specificity	F-Score
Meningioma	**0.9183**	0.9637	0.9433	0.9894	0.9534
Glioma	**0.9183**	**0.9921**	0.8807	**0.9939**	0.9331
Pituitary	**0.9183**	0.9780	**0.9570**	0.9906	**0.9674**

Table 4.12. Performance metrics when threshold is 0.5

Reference Class	Accuracy	Precision	Sensitivity	Specificity	F-Score
Meningioma	**0.9314**	0.9710	0.9504	0.9915	0.9606
Glioma	**0.9314**	**0.9923**	0.9053	**0.9939**	0.9468
Pituitary	**0.9314**	0.9834	**0.9570**	0.9930	**0.9700**

It should also be noted that different exceptional cases have occurred for some of the test samples. These cases may be collected into three categories:

a) Both tumor location and class are true but there is an extra anchor box
b) Tumor class is correct but the tumor is not located
c) Both tumor location and class are true but a large tumor is detected as two different tumors

A sample image for each of these case are is shown in Figure 4.2. All of these samples are considered as a correct classification when constructing the confusion matrices.

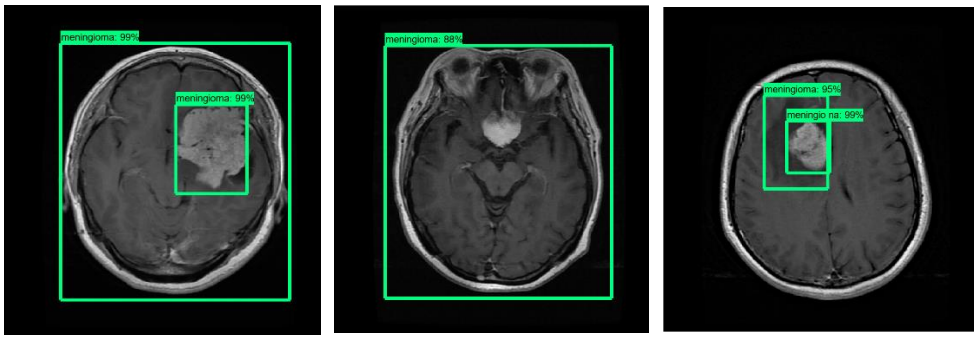

(a) (b) (c)

Figure 4.2. Samples for Exceptional Test Cases

The dataset used in this work is publicly available. Thus, four other previous works have been found in the literature that applies various deep learning techniques on this dataset. In Table 4.13, the results obtained in these works are summarized and compared with the ones in this work. Performance of one of the works [3] is higher than the proposed method. However, in that work a series of convolution and pooling steps followed by a fully connected layer is used for feature extraction. Then using these features, an Exterme Learning Machine (ELM) model is trained. In other words, that method utilizes initial steps of CNN for generating feautre vectors but the trained model is something different than CNN.

Table 4.13. Previous Works that Applies Various Deep Learning Techniques on This Dataset.

Reference no	**Year**	**Classification Method**	**Performance Metric**	**Obtained result**	**This work**
1	2018	LinkNet	F-score	0.7900	0.9700
2	2018	CapsNet	Accuracy	0.9089	0.9314
3	2018	Kernel Extreme Learning Machines (KE-CNN)	Accuracy	0.9368	0.9314
			Precision	0.9830	0.9923
			Sensitivity	1.0000	0.9570
			F-Score	0.9910	0.9700
5	2017	CNN	Accuracy	0.9143	0.9314

5. CONCLUSION AND FUTURE WORK

In this study, MRI brain images are used for detection of tumors using faster R-CNN method. A model is trained using 2452 images containing three types of tumors. It may be concluded that faster R-CNN is suitable algorithm for this problem as the achieved classification accuracy is 93.14% which is higher than the related work using the same dataset. Also, it has been observed that some of the tumors are correctly detected with low scores. Therefore, the results are evaluated using three different levels of detection scores. Among the three types of tumors, Glioma has the lowest detection rate with a sensitivity of 90.53% and Pituitary has the highest rate with a sensitivity of 95.70%. Since only one test sample is predicted as false positive for Glioma class, the precision value of the Glioma is the highest, on the other hand high number of false negative samples causes its sensitivity value to be low. The presence of unclassified samples is something related to detections with low scores. Such samples may be thought to be classified as "*no tumors*" even though they contain a tumor. This situation may be overcome by adding healthy images (i.e. images containing no tumors) to the dataset as the fourth class.

The dataset used in this work is publicly available. The previous work using the same dataset have carefully been investigated and the related results have been compared. Among the related papers using deep learning methods for detection, the results obtained in this study are the found to be the best one.

As can be seen from Section 3, a set of constant parameters has been used for generating the CNN model. In the future, some optimization algorithms (such as genetic algorithm, particle swarm optimization, simulated annealing, etc…) may be utilized to find the best parameter set giving the highest classification accuracy. Also, this method may be applied to images taken from different parts of the body to detect tumors in the other tissue.

REFERENCES

A Beginner's Guide to Convolutional Neural Networks (CNNs). (2019). Retrieved 5 August 2019, from https://skymind.ai/wiki/convolutional-network

A Comprehensive Guide to Convolutional Neural Networks — the ELI5 way. (2019). Retrieved 5 August 2019, from https://towardsdatascience.com/a-comprehensive-guide-to-convolutional-neural-networks-the-eli5-way-3bd2b1164a53

Akram M. U., and Usman, A., 2011. "Computer Aided System for Brain Tumor Detection and Segmentation", IEEE, International Conference on Computer Networks & Information Technologies (ICCNIT), pp. 299-302.

Alfonse, M., and Salem M., 2016. An Automatic Classification of Brain Tumors through MRI Using Support Vector Machine. Egypt Comput Sci J 40:11–21.

Babu, V. T., and Begum, S., 2015. "An Adaptive MRI Tumor Detection Using Neural Network Based Adaboost Algorithm", International Journal of Computer Science and Information Technologies, Vol. 6 (1).

Behzadfar N., and Soltanian-Zadeh, H., 2012. "Automatic Segmentation of Brain Tumors in Magnetic Resonance Images", International Conference on Biomedical and Health Informatics, IEEE, pp.329-332.

Bhattacharyya D., and Kim, T., 2011." Brain Tumor Detection Using MRI Image Analysis" © Springer-Verlag Berlin Heidelberg.

Bjoern, M. et al., 2015. The Multi-Modal Brain Tumor Image Segmentation Benchmark (BraTS). IEEE Trans. Med. Imaging 34(10), 1993–2024.

Brain Tumor - Introduction. (2019). Retrieved 5 August 2019, from https://www.cancer.net/cancer-types/brain-tumor/introduction

Chato L., and Latifi, S., 2017. "Machine Learning and Deep Learning Techniques to Predict Overall Survival of Brain Tumor Patients using MRI Images," 2017

IEEE 17th International Conference on Bioinformatics and Bioengineering (BIBE), Washington, DC, pp. 9-14. doi: 10.1109/BIBE.2017.00-86.

Chen, L., Papandreou, G., Kokkinos, I., Murphy, K., and Yuille, A. L., 2018. Deeplab: Semantic Image Segmentation with Deep Convolutional Nets, Atrous Convolution, and Fully Connected CRFs. IEEE Transactions on Pattern Analysis and Machine Intelligence, 40(4):834–848.

Chen, L., Wu, Y., DSouza, A. M., Abidin, A. Z., Wismuller, A., and Xu, C., 2018. MRI Tumor Segmentation with Densely Connected 3D CNN. In Medical Imaging 2018: Image Processing, volume 10574, page 105741F. International Society for Optics and Photonics.

Cheng J. et al., 2015. "Enhanced Performance of Brain Tumor Classification via Tumor Region Augmentation and Partition," PloS one, vol. 10, no. 10, p. e0140381.

Cullen, N. C., and Avants, B. B., 2018. Convolutional Neural Networks for Rapid and Simultaneous Brain Extraction and Tissue Segmentation. In Brain Morphometry, pages 13–34. Springer.

CS 230 - Convolutional Neural Networks Cheatsheet. 2019. Retrieved 6 August 2019, from https://stanford.edu/~shervine/teaching/cs-230/cheatsheet-convolutional-neural-networks.

Deepa and Singh, A., 2016. "Review of Brain Tumor Detection from MRI Images", 2016 3rd International Conference on Computing for Sustainable Global Development (INDIACom), New Delhi, pp. 3997-4000.

Demirhan, A., and Güler, I., 2014. Using Wavelet Transform and Neural Networks For the Analysis of Brain MR Images. IEEE 18.Sinyal Isleme ve Iletisim Uygulamaları Kurultayı.

Ezhilarasi, R. and Varalakshmi, P., 2018. Tumor Detection in the Brain Using Faster R-CNN. Proceedings of the Second International Conference on I-SMAC. ISBN:978-1-5386-1442-6.

Federer, L. et al., 2018. Data Sharing in PLOS ONE: An Analysis of Data Availability Statements. PLOS ONE, vol. 13, no. 5, p. e0194768. Available: 10.1371/journal.pone.0194768.

Gadpayleand, P., and Mahajani, P. S., 2013."Detection and Classification of Brain Tumor in MRI Images ", International Journal of Emerging Trends in Electrical and Electronics, IJETEE – ISSN: 2320-9569, Vol. 5, Issue. 1.

Ghanavati, S., Li, J., Liu, T., Babyn, P. S., Doda, W., and Lampropoulos, G., 2012. "Automatic Brain Tumor Detection In Magnetic Resonance Images" IEEE.

Glioma - Symptoms and causes. (2019). Retrieved 5 August 2019, from https://www.mayoclinic.org/diseases-conditions/glioma/symptoms-causes/syc-20350251

Goswami, S., and Bhaiya, L., 2013. " Brain Tumor Detection Using Unsupervised Learning based Neural Network", IEEE International Conference on Communication Systems and Network Technologies.

Haritha, D., 2016. "Comparative Study on Brain Tumor Detection Techniques", International Conference on Signal Processing, Communication, Power and Embedded System (SCOPES).

Havaei M. et al., 2017. Brain Tumor Segmentation with Deep Neural Networks. Medical Image Analysis, vol. 35, pp. 18-31, Available: 10.1016/j.media.2016.05.004.

How Deep Learning Can Help Prevent Financial Fraud. (2019). Retrieved 5 August 2019, from https://www.investopedia.com/terms/d/deep-learning.asp

Ibrahim, W. H., Osman, A., and Mohamed Y. I., 2013."MRI Brain Image Classification Using Neural Networks", IEEE International Conference On Computing, Electrical and Electronics Engineering, ICCEEE.

ImageNet. (2019). Retrieved 5 August 2019, from http://www.image-net.org/

Iqbal, S., Ghani, M. U., Saba, T., and Rehman, A., 2018. Brain Tumor Segmentation in Multi-Spectral MRI Using Convolutional Neural Networks (CNN). Microscopy Research and Technique, 81(4):419–427.

Isensee, F., Kickingereder, P., Bonekamp, D., Bendszus, M., Wick, W., Schlemmer, H. P., Maier-Hein, K., 2017. Brain Tumor Segmentation Ssing Large Receptive Field Deep Convolutional Neural Networks. Bildverarbeitung f¨ur die Medizin 2017. Informatik aktuell, pp. 86–91. Springer, Heidelberg. https://doi.org/10.1007/ 978-3-662-54345-0 24

Işın, A., Direkoğlu, C. and Şah, M., 2016. Review of MRI-based Brain Tumor Image Segmentation Using Deep Learning Methods. Procedia Computer Science, vol. 102, pp. 317-324, Available: 10.1016/j.procs.2016.09.407.

John, P., 2012. "Brain Tumor Classification Using Wavelet and Texture Based Neural Network," International Journal of Scientific & Engineering Research, vol. 3, no. 10, pp. 1-7.

Joshi, D. M., Rana, N. K., and Misra, V. M., 2010. " Classification of Brain Cancer Using Artificial Neural Network" , IEEE International Conference on Electronic Computer Technology, ICECT.

Kamnitsas, K., Chen, L., Ledig, C., Rueckert, D., Glocker, B., 2015. Multi-scale 3D Convolutional Neural Networks for Lesion Segmentation in Brain MRI. Ischemic Stroke Lesion Segmentation 13, 46.

Kamnitsas, K., Ledig, C., Newcombe, V.F., Simpson, J.P., Kane, A.D., Menon, D.K., Rueckert, D., Glocker, B., 2017. Efficient Multi-scale 3D CNN with Fully Connected CRF for Accurate Brain Lesion Segmentation. Med. Image Anal. 36, 61–78.

Kumar M., and Mehta, K. K., 2011. “A Texture Based Tumor Detection and Automatic Segmentation Using Seeded Region Growing Method”, International Journal of Computer Technology and Applications.

Kumar, P., and Vijayakumar, B., 2015. Brain Tumor MR Image Segmentation and Classification Using by PCA and RBF Kernel Based Support Vector Machine. Middle East J Sci Res 23(9):2106–2116.

LeCun, Y., Bengio, Y., Hinton, G., 2015. Deep Learning. Nature. 521. 436-44. 10.1038/nature14539.

Long, J., Shelhamer, E., Darrell, T., 2015. Fully Convolutional Networks for Semantic Segmentation. In: Proceedings of the IEEE Conference on Computer Vision and Pattern Recognition, pp. 3431–3440.

Meenakshi R., and Anandhakumar, P., 2012. "Brain Tumor Identification in MRI with BPN Classifier and Orthonormal Operators", European Journal of Scientific Research.

Meningioma - Symptoms and causes. (2019). Retrieved 5 August 2019, from https://www.mayoclinic.org/diseases-conditions/meningioma/symptoms-causes/syc-20355643

Neuroendocrine Tumors - Introduction. (2019). Retrieved 5 August 2019, from https://www.cancer.net/cancer-types/neuroendocrine-tumors/introduction

Nilakshi, D., and Bhattacharyya, K., 2018. Automatic Brain Tumor Detection and Classification of Grades of Astrocytoma. Lecture Notes in Networks and Systems. 10.1007/978-981-10-6890-4_11.

Ouseph, C. N., and Shruti, K., 2016. " A Reliable Method for Brain Tumor Detection Using Cnn Technique "IOSR Journal of Electrical and Electronics Engineering (IOSR-JEEE).

Pan, Y. et al., 2015. "Brain Tumor Grading Based on Neural Networks and Convolutional Neural Networks," in Engineering in Medicine and Biology Society (EMBC), 2015 37th Annual International Conference of the IEEE, pp. 699-702: IEEE. 319.

Pereira, S., Pinto, A., Alves, V., and Silva, C. A., 2016. " Brain Tumor Segmentation Using Convolutional Neural Networks in MRI Images "IEEE Transactions on Medical Imaging, Vol. 35, No. 5, 1240-1251.

Pituitary tumors - Symptoms and causes. (2019). Retrieved 5 August 2019, from https://www.mayoclinic.org/diseases-conditions/pituitary-tumors/symptoms-causes/syc-20350548

Prabin A., and Veerappan, J., 2014. "Computer Assisted Diagnosis of Brain Tumor in MRI Image Using Texture Features as Input to AdaBoost Classifier",

Research Journal of Applied Sciences, Engineering and Technology 8(24): 2374-2380.

Pramanik, S., Bhattacharjee, D., and Nasipuri, M., 2015. "Wavelet Based Thermogram Analysis for Breast Cancer Detection", Int. Symp. On Advanced Computing and Communication (ISACC), Silchar, India, pp. 205-212, DOI: 10.1109/ISACC.2015.7377343.

Prasoon, A. et al., 2013. Deep Feature Learning for Knee Cartilage Segmentation Using a Triplanar Convolutional Neural Network. MICCAI, pp. 246–253.

Quora. (2019). Retrieved 6 August 2019, from https://www.quora.com/What-is-max-pooling-in-convolutional-neural-networks.

Radiation Oncology Branch, 2018. Brain Tumor Segmentation in MRI Scans Using Deeply-Supervised Neural Networks. In Brainlesion: Glioma, Multiple Sclerosis, Stroke and Traumatic Brain Injuries: Third International Workshop, BrainLes 2017, Held in Conjunction with MICCAI 2017, Quebec City, QC, Canada, September 14, 2017, Revised Selected Papers, volume 10670, page 320. Springer.

Rathi, V. P., and Palani, S., 2015. “Brain Tumor Detection and Classification Using Deep Learning Classifier on MRI Images,” Research Journal of Applied Sciences, Engineering and Technology, vol. 10, no. 2, doi: 177-187.

Ronneberger, O., Fischer, P., Brox, T., 2015. U-Net: Convolutional Networks for Biomedical Image Segmentation. In: Navab, N., Hornegger, J., Wells, W.M., Frangi, A.F. (eds.) MICCAI 2015. LNCS, vol. 9351, pp. 234–241. Springer, Cham. https://doi.org/10.1007/978-3-319-24574-4 28.

Roy S., and Bandyopadhyay, S. K., 2012. “Detection and Quantification of Brain Tumor from MRI of Brain and its Symmetric Analysis”, International Journal of Information and Communication Technology Research, KY, USA.

Sachdeva J. et al., 2013. “Segmentation, Feature Extraction, and Multiclass Brain Tumor Classification.” J. of Digital Imaging, vol. 26, no. 6, pp. 1141–1150, doi: 10.1007/s10278-013-9600-0.

Selvakumar, J., Lakshmi, A., and Arivoli, T., 2012. Brain Tumor Segmentation and Its Area Calculation in Brain MR Images Using K-mean Clustering and Fuzzy C-mean Algorithm.

Sharma, K., and Kaur, N., 2013. " Comparative Analysis of Various Edge Detection Techniques", International Journal of Advanced Research in Computer Science and Software Engineering, IJARCSSE, ISSN: 2277 128X, Volume 3, Issue 12.

Shree, N. V., and Kumar, T., 2018. Identification and Classification of Brain Tumor MRI Images with Feature Extraction Using DWT and Probabilistic Neural Network. Brain Informatics, vol. 5, no. 1, pp. 23-30, Available: 10.1007/s40708-017-0075-5.

Sun, W., Zheng, B. and Qian, W. 2017. Automatic Feature Learning Using Multichannel ROI Based on Deep Structured Algorithms for Computerized Lung Cancer Diagnosis. Computers in Biology and Medicine, vol. 89, pp. 530-539, Available: 10.1016/j.compbiomed.2017.04.006.

TensorFlow TensorFlow. (2019). Retrieved 5 August 2019, from https://www.tensorflow.org/

Tensorflow. (2019). Retrieved 5 August 2019, from https://www.usenix.org/system/files/conference/osdi16/osdi16-abadi.pdf

Tzutalin/labelImg. (2019). Retrieved 5 August 2019, from https://github.com/tzutalin/labelimg

Urban, G. et al., 2014. Multi-modal Brain Tumor Segmentation using Deep Convolutional Neural Networks. MICCAI BraTS (Brain Tumor Segmentation) Challenge. Proceedings, winning contribution, pp. 31–35.

Urban, G., Bendszus, M., Hamprecht, F., and Kleesiek, J, 2014. Multi-modal Brain Tumor Segmentation Using Deep Convolutional Neural Networks. MICCAI

BraTS (Brain Tumor Segmentation) Challenge. Proceedings, winning contribution, pages 31–35.

Wachinger, C., Reuter, M., and Klein, T., 2018. Deepnat: Deep Convolutional Neural Network for Segmenting Neuroanatomy. NeuroImage, 170:434–445.

WHO Cancer Control Programme. (2019). Retrieved 5 August 2019, from https://www.who.int/cancer/en/

Yu H. and Fan, J. L., 2008. "Three-level Image Segmentation Based on Maximum Fuzzy Partition Entropy of 2-D Histogram and Quantum Genetic Algorithm", Advanced Intelligent Computing Theories and Applications. With Aspects of Artificial Intelligence. Lecture Notes in Computer Science, Berlin, Heidelberg.

Yu, F., Koltun, V., 2016. Multi-scale Context Aggregation by Dilated Convolutions. In: International Conference on Learning Representations (ICLR). arXiv: 1511.07122v3.

Yu, F., Koltun, V., Funkhouser, T., 2017. Dilated Residual Networks. In: Computer Vision and Pattern Recognition (CVPR). arXiv: 1705.09914

Zhang, Q. et al., 2016. Deep Learning Based Classification of Breast Tumors with Shear-wave Elastography. Ultrasonics, vol. 72, pp. 150-157, Available: 10.1016/j.ultras.2016.08.004.

Zhao, X., Wu, Y., Song, G., Li, Z., Zhang, Y., and Fan, Y., 2018. A Deep Learning Model Integrating FCNNs and CRFs for Brain Tumor Segmentation. Medical Image Analysis, 43:98–111.

CURRICULUM VITAE

Kerem SALÇIN was born in Adana, in 1992. He graduated from Adana Genç İş Adamları Derneği Primary School in 2006. He graduated from Adana Ticaret Odası Anatolian High School in 2010. He graduated Electrical and Electronics Engineering bachelor degree at Çukurova University in 2015. He graduated from Master of Business Administration (MBA) at Çukurova University in 2017.